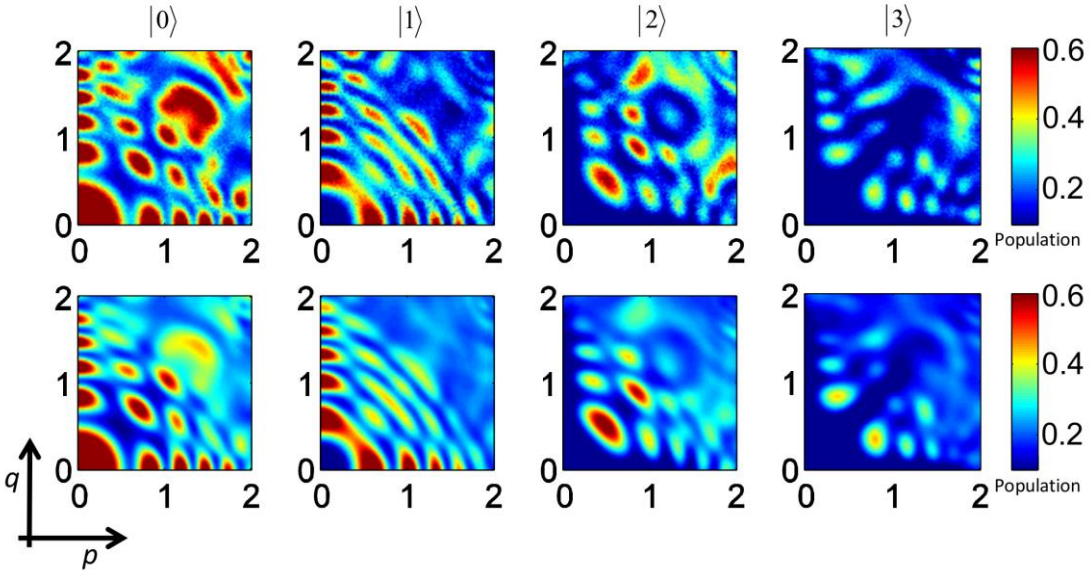

Supplementary Figure 1. Experiment and simulation with finite qudit anharmonicity. (**a**), Experimental data taken after a 60 ns three-tone pulse. (**b**), Simulation using the Hamiltonian (1).

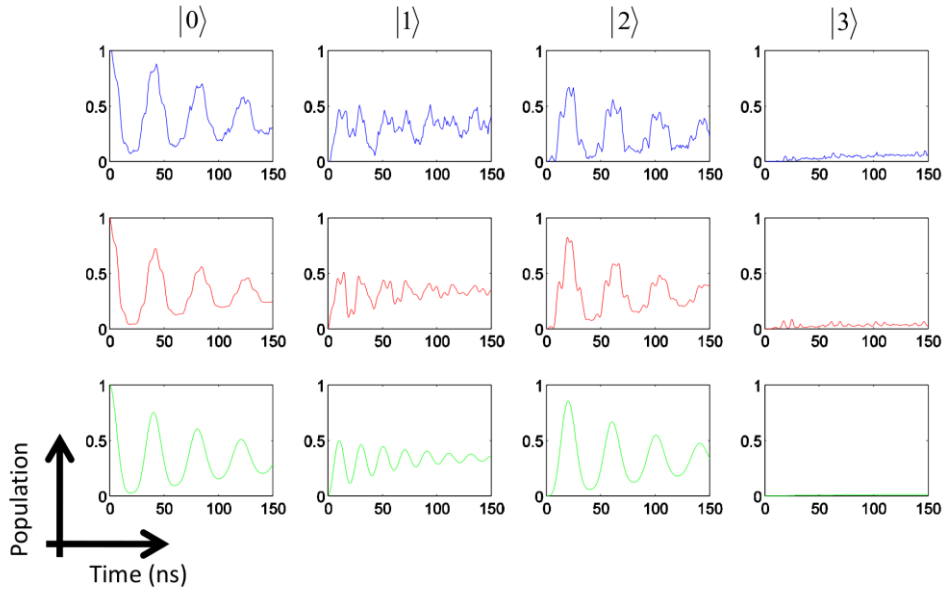

Supplementary Figure 2. Pythagorean dynamics in the time domain. (**a**), Experimental data. The three-tone pulse is generated with p=q=0.86. (**b**), Simulation

with finite anharmonicity. Jagged features are seen to be coherent SU(4) effects. (**c**), Simulation with infinite anharmonicity. Populations oscillate smoothly.

Supplementary Note 1

In this section we show how finite anharmonicity prevents confinement of qudit dynamics to SO(4) rotations and show additional experimental data of the SU(4) dynamics and related numerical simulations.

The impact of finite anharmonicity on the dynamical symmetry is a general feature of multi-level systems. In our experiment the four-level qudit is driven by a three-tone pulse $V = V_{01}\cos(\omega_{01}t) + \frac{V_{12}}{\sqrt{2}}\cos(\omega_{12}t) + \frac{V_{23}}{\sqrt{3}}\cos(\omega_{23}t)$ which produces the following Hamiltonian:

$$H = \begin{pmatrix} 0 & V & 0 & 0 \\ V^* & \varepsilon_1 & \sqrt{2}V & 0 \\ 0 & \sqrt{2}V^* & \varepsilon_2 & \sqrt{3}V \\ 0 & 0 & \sqrt{3}V^* & \varepsilon_3 \end{pmatrix} . \qquad (1)$$

In the interaction picture, this becomes

$$H = \frac{1}{2}\begin{pmatrix} 0 & V_{01} & 0 & 0 \\ V_{01}^* & 0 & V_{12} & 0 \\ 0 & V_{12}^* & 0 & V_{23} \\ 0 & 0 & V_{23}^* & 0 \end{pmatrix} + H' \qquad (2)$$

where the off-resonant matrix is

$$H' = \frac{1}{2}\begin{pmatrix} 0 & 0 & 0 & 0 \\ 0 & 0 & \sqrt{2}V_{01}e^{-i(\omega_{01}-\omega_{12})t} & 0 \\ 0 & \sqrt{2}V_{01}^*e^{i(\omega_{01}-\omega_{12})t} & 0 & \sqrt{3}V_{01}e^{-i(\omega_{01}-\omega_{23})t} \\ 0 & 0 & \sqrt{3}V_{01}^*e^{i(\omega_{01}-\omega_{23})t} & 0 \end{pmatrix}$$

$$+\frac{1}{2}\begin{pmatrix} 0 & \frac{1}{\sqrt{2}}V_{12}e^{-i(\omega_{12}-\omega_{01})t} & 0 & 0 \\ \frac{1}{\sqrt{2}}V_{12}^{*}e^{i(\omega_{12}-\omega_{01})t} & 0 & 0 & 0 \\ 0 & 0 & 0 & \sqrt{\frac{3}{2}}V_{12}e^{-i(\omega_{12}-\omega_{23})t} \\ 0 & 0 & \sqrt{\frac{3}{2}}V_{12}^{*}e^{i(\omega_{12}-\omega_{23})t} & 0 \end{pmatrix}$$

$$+\frac{1}{2}\begin{pmatrix} 0 & \frac{1}{\sqrt{3}}V_{23}e^{-i(\omega_{23}-\omega_{01})t} & 0 & 0 \\ \frac{1}{\sqrt{3}}V_{23}^{*}e^{i(\omega_{23}-\omega_{01})t} & 0 & \sqrt{\frac{2}{3}}V_{23}e^{-i(\omega_{23}-\omega_{12})t} & 0 \\ 0 & \sqrt{\frac{2}{3}}V_{23}^{*}e^{i(\omega_{23}-\omega_{12})t} & 0 & 0 \\ 0 & 0 & 0 & 0 \end{pmatrix}. \qquad (3)$$

At the limit of large anharmonicity relative to the drive, the dynamical averaging of this matrix is zero and we immediately recover the reduction to SO(4) Pythagorean control, as discussed in the main text.

Supplementary Figure 1a shows experimental data obtained from measurement and Supplementary Figure 1b shows simulation using the Hamiltonian (2). Even minor, asymmetric features are reproduced very well. We note that a better quantitative match is achieved when longer coherence times are used in simulation, implying echoing of some qudit coherences by the strong three-tone pulse which is not taken into account in our simulation. All simulations are done on a six-level system and confirm that only the first four levels participate in the dynamics.

At large amplitudes, results are found to depend on the relative phases between the three frequency components of the drive. If the dynamics were SO(4), such phases would only define the subspace of SU(4) in which the qudit undergoes SO(4)

rotations, and no effect of these relative phases would be measured. The sensitivity to these phases indicates that the dynamics in this regime are indeed SU(4) .

The success of simulation with (2) can also be seen when comparing to time-domain measurements. Supplementary Figure 2a shows time-domain evolution of the qudit population for p=q=0.86, Supplementary Figure 2b shows simulation with (2) and Supplementary Figure 2c shows simulation with the large-anharmonicity Hamiltonian. The effect of the finite anharmonicity is apparent, and even small, jagged features in the experimental data are seen to be coherent, not noisy, dynamics.

Supplementary Note 2

As shown in the previous section, a multi-tone drive in conjunction with finite anharmonicity results in off-resonant couplings, i.e. the operator H' of Eq. (3). Any one of the three components of H' can be made time-independent by transforming to a suitable rotating frame, but this would leave the other components oscillating at a beat frequency. Although the full Hamiltonian cannot be made time-independent for this reason, we can understand how the finite anharmonicity leads to SU(4) dynamics by studying the group-theoretical aspects of the detuned Hamiltonian, which are frame-independent.

We generalize the Bell-frame analysis of a four-level system to allow detuning between the drives and their associated transitions, starting with a general time-independent Hamiltonian of the form:

$$H = \begin{pmatrix} 0 & V_{01} & iV_{02} & V_{03} \\ V_{01} & \Delta_1 & V_{12} & iV_{13} \\ -iV_{02} & V_{12} & \Delta_2 & V_{23} \\ V_{03} & -iV_{13} & V_{23} & \Delta_3 \end{pmatrix}, \qquad (4)$$

where all the parameters are real-valued (i.e. $V_{ij} = V_{ji}$). Any one of the components of H' of Eq. (2) can be brought into this form, but not all three simultaneously.

Applying the unitary transformation $H_{\mathrm{B}} = W^{-1} H W$, where

$$W = \frac{1}{\sqrt{2}} \begin{pmatrix} 1 & 0 & 0 & 1 \\ 0 & 1 & 1 & 0 \\ 0 & 1 & -1 & 0 \\ 1 & 0 & 0 & -1 \end{pmatrix}, \qquad (5)$$

produces the Bell-frame Hamiltonian

$$H_{\mathrm{B}} = \begin{pmatrix} \Delta_3 + 2V_{03} & V_{01} + V_{23} + i(V_{02} - V_{13}) & V_{01} - V_{23} + i(V_{02} + V_{13}) & -\Delta_3 \\ V_{01} + V_{23} - i(V_{02} - V_{13}) & \Delta_1 + \Delta_2 + 2V_{12} & \Delta_1 - \Delta_2 & V_{01} - V_{23} + i(V_{02} + V_{13}) \\ V_{01} - V_{23} - i(V_{02} + V_{13}) & \Delta_1 - \Delta_2 & \Delta_1 + \Delta_2 - 2V_{12} & V_{01} + V_{23} + i(V_{02} - V_{13}) \\ -\Delta_3 & V_{01} - V_{23} - i(V_{02} + V_{13}) & V_{01} + V_{23} - i(V_{02} - V_{13}) & \Delta_3 - 2V_{03} \end{pmatrix} . \quad (6)$$

This Hamiltonian can be decomposed into tensor products of SU(2) operators as follows:

$$\begin{aligned} H_{\mathrm{B}} = & \frac{V_{01} + V_{23}}{2} \sigma_x^{(1)} \times I^{(2)} + \frac{V_{02} - V_{13}}{2} \sigma_y^{(1)} \times I^{(2)} + \frac{V_{03} + V_{12}}{2} \sigma_z^{(1)} \times I^{(2)} \\ & + \frac{V_{01} - V_{23}}{2} I^{(1)} \times \sigma_x^{(2)} + \frac{V_{02} + V_{13}}{2} I^{(1)} \times \sigma_y^{(2)} + \frac{V_{03} - V_{12}}{2} I^{(1)} \times \sigma_z^{(2)} \\ & + \frac{\Delta_1 + \Delta_2 + \Delta_3}{2} I^{(1)} \times I^{(2)} + \frac{\Delta_1 - \Delta_2 - \Delta_3}{2} \sigma_x^{(1)} \times \sigma_x^{(2)} + \frac{-\Delta_1 + \Delta_2 - \Delta_3}{2} \sigma_y^{(1)} \times \sigma_y^{(2)} \\ & + \frac{-\Delta_1 - \Delta_2 + \Delta_3}{2} \sigma_z^{(1)} \times \sigma_z^{(2)} \end{aligned} \qquad (7)$$

The above is an explicit example of Cartan's decomposition in SU(4) , which states that any unitary transformation in SU(4) can be written as the product of three elements $U = K_1 A K_2$, where K_1 and K_2 are local manipulations of qubits 1 and 2, respectively, i.e.

Local qubit 1: $\sigma_x^{(1)} \times I^{(2)}, \sigma_y^{(1)} \times I^{(2)}, \sigma_z^{(1)} \times I^{(2)}$

Local qubit 2: $I^{(1)} \times \sigma_x^{(2)}, I^{(1)} \times \sigma_y^{(2)}, I^{(1)} \times \sigma_z^{(2)}$

and A is of the form:

$$A = e^{-\alpha_1 \sigma_x^{(1)} \times \sigma_x^{(2)}} e^{-\alpha_2 \sigma_y^{(1)} \times \sigma_y^{(2)}} e^{-\alpha_3 \sigma_z^{(1)} \times \sigma_z^{(2)}},$$

where $\sigma_x^{(1)} \times \sigma_x^{(2)}$, $\sigma_y^{(1)} \times \sigma_y^{(2)}$, $\sigma_z^{(1)} \times \sigma_z^{(2)}$ are *non-local* operators that sit in $\frac{\mathrm{SU}(4)}{\mathrm{SU}(2) \otimes \mathrm{SU}(2)}$.

This decomposition is also called the "KAK decomposition" and spans the SU(4) dynamical space.

We note that the off-diagonal coupling terms $\{V_{ij}\}$ belong to the local transformations, while the detunings belong to the non-local transformations. Detuning the drive thus switches the dynamics between SO(4) and SU(4).

Consequently, our experimental results (and associated simulations) for higher-power drives indicate the simultaneous action of several non-commuting Hamiltonians, thus leading to the interference of Pythagorean dynamics along with coupling oscillations, as presented in Fig. 3 of the main text.